BIOCHEMISTRY
including biophysical chemistry & molecular biology

Article

pubs.acs.org/biochemistry

# DEAD-Box Helicases Form Nucleotide-Dependent, Long-Lived Complexes with RNA

Fei Liu,[†,‡,§,⊥] Andrea A. Putnam,[‡,§] and Eckhard Jankowsky*[,‡,§,⊥]

[†]College of Veterinary Medicine, Nanjing Agricultural University, Nanjing, Jiangsu, 210095, China

[‡]Center for RNA Molecular Biology, School of Medicine, [§]Department of Biochemistry, School of Medicine, [⊥]Department of Physics, College of Arts and Sciences Case Western Reserve University, 10900 Euclid Avenue, Cleveland, Ohio 44106

**ABSTRACT:** DEAD-box RNA helicases bind and remodel RNA and RNA−protein complexes in an ATP-dependent fashion. Several lines of evidence suggest that DEAD-box RNA helicases can also form stable, persistent complexes with RNA in a process referred to as RNA clamping. The molecular basis of RNA clamping is not well understood. Here we show that the yeast DEAD-box helicase Ded1p forms exceptionally long-lived complexes with RNA and the nonhydrolyzable ATP ground-state analogue ADP-$BeF_x$ or the nonhydrolyzable ATP transition state analogue ADP-$AlF_x$. The complexes have lifetimes of several hours, and neither nucleotide nor $Mg^{2+}$ is released during this period. Mutation of arginine 489, which stabilizes the transition state, prevents formation of long-lived complexes with the ATP transition state analogue, but not with the ground state analogue. We also show that two other yeast DEAD-box helicases, Mss116p and Sub2p, form comparably long-lived complexes with RNA and ADP-$BeF_x$. Like Ded1p, Mss116p forms long-lived complexes with ADP-$AlF_x$, but Sub2p does not. These data suggest that the ATP transition state might vary for distinct DEAD-box helicases, or that the transition state triggers differing RNA binding properties in these proteins. In the ATP ground state, however, all tested DEAD-box helicases establish a persistent grip on RNA, revealing an inherent capacity of the enzymes to function as potent, ATP-dependent RNA clamps.

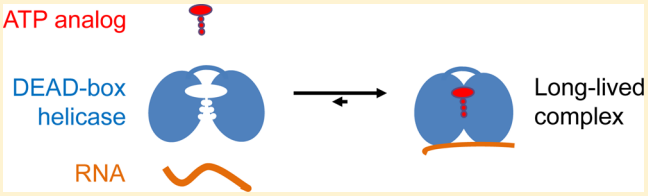


Nearly all aspects of eukaryotic RNA metabolism involve DEAD-box RNA helicases.[1] These enzymes bind and remodel RNA and RNA−protein complexes in an ATP-dependent fashion.[2,3] Observations with the DEAD-box helicase eIF4A-III (DDX48) have raised the possibility that DEAD-box helicases might also function as ATP-dependent RNA clamps.[4−8] The term RNA clamp describes persistent, immobile RNA binding by the helicase.[1]

EIF4A-III hydrolyzes ATP and unwinds RNA duplexes in an ATP-dependent fashion,[5] but in the cell eIF4A-III functions as an ATP-dependent, immobile RNA adaptor for the exon junction complex (EJC), an assembly of several proteins.[9] eIF4A-III binds RNA in an ATP-dependent fashion, while other EJC factors bind to eIF4A-III and arrest its ATP hydrolysis cycle, thus creating a stable eIF4A-III−RNA complex.[9−12]

It has been speculated that other DEAD-box proteins might also play roles as RNA clamps,[6−8] but no direct evidence for this notion has been published. Kinetic investigation of the RNA-stimulated ATP hydrolysis reaction by the DEAD-box helicases DbpA and Mss116p suggested that ATP binding, prior to its hydrolysis, induces stable enzyme−RNA complexes.[13,14] While these observations raised the possibility that ATP-dependent "RNA clamping" might be a common feature of DEAD-box RNA helicases, the critical long-lived ATP-dependent complexes between RNA and DEAD-box helicases have not been observed and examined directly. It is thus unknown whether such complexes indeed exist in the absence of other protein cofactors, how stable and long-lived these complexes are, whether ATP and the required metal remain bound continuously, which states of the ATP hydrolysis cycle promote stable complex formation, and whether many or even all DEAD-box helicases can form such complexes.

Here we address these questions. We directly examine biochemical properties of nucleotide-dependent, long-lived complexes between RNA and three different DEAD-box helicases from *Saccharomyces cerevisiae*. We show that Ded1p, Mss116p, and Sub2p form exceptionally long-lived complexes with RNA and the nonhydrolyzable ATP ground-state ADP-$BeF_x$. The complexes have lifetimes of several hours, and neither nucleotide nor $Mg^{2+}$ is released during this period. Ded1p and Mss116p, but not Sub2p, form comparably long-lived complexes with RNA and the nonhydrolyzable ATP transition-state analogue ADP-$AlF_x$. Mutation of a critical arginine in Ded1p (R489A) that stabilizes the transition state prevents formation of long-lived complexes with the transition-state analogue but not with the ground-state analogue. Our data collectively show that the DEAD-box helicases tested here can establish a persistent grip on RNA in the ATP ground state. This observation reveals an inherent capacity of DEAD-box proteins to function as potent, ATP-dependent RNA clamps. The data further suggest that the ATP transition state might

**Received:** November 15, 2013
**Revised:** December 23, 2013
**Published:** December 24, 2013

   dx.doi.org/10.1021/bi401540q | *Biochemistry* 2014, 53, 423−433

vary for distinct DEAD-box helicases or that the transition state triggers differing RNA binding properties in these proteins.

## MATERIALS AND METHODS

**Materials.** Ded1p, Mss116p, and Sub2p were expressed and purified as described.[15,16,45] RNA oligonucleotides were purchased from Dharmacon (Lafayette, CO), and radiolabeled substrate was prepared as previously described.[17] Substrate sequences were as follows: 10 nt single-strand RNA: 5′-AGC ACC GUA A-3′, ssRNA scavenger (73 nt) 5′-CCGUA-CAGGCUCUGGGUACAAUGCUUGUUUUUUUU-CUGUCUGGGACGUA CUGCAUCAAUGACAUCAGC-AUCAA-3′. Fluorescently labeled and biotinylated oligonucleotides were also purchased from Dharmacon. Substrate sequences were as follows (underlined regions corresponding to the duplex region): 3′-Cy3-AACUACGACUACAGUAAC-UACGACCGACGCAGAAAUGCCACGA-5′ and 3′-Bio-UUUCGUGGCAUUUCUGCGUCG-Cy5-5′. The extent of fluorescent labeling was verified by UV spectroscopy and found to be greater than 80% according to extinction coefficients of the RNA and fluorophores.[18] The Cy3 labeled strand was mixed with the biotinylated and Cy5 labeled strand in a 2:1 ratio. RNAs were heated to 95 °C for 2 min, cooled down to room temperature over approximately 30 min, and stored at −20 °C.

ADP-$BeF_x$ and ADP-$AlF_x$ were prepared as a mixture of ADP (Sigma) with 5-fold excess of the corresponding metal fluorides, and a 25-fold molar excess of NaF (Arcos Organics).[19] ADPNP was purchased from SIGMA, and EDTA was purchased from Fischer Scientific.

**RNA−Protein Binding Reactions.** RNA−protein binding reactions (10 μL for reactions in Figure 1, 30 μL for reactions used to determine dissociation rate constants, Table 1) were assembled in a temperature-controlled aluminum block at 19 °C in a buffer containing 40 mM Tris-HCl (pH 8.0), 50 mM NaCl, 0.5 mM $MgCl_2$, 2 mM DTT, 1 U·μL$^{-1}$ RNasin, 0.01% (v/v) Nonidet P-40, 0.5 nM radiolabeled RNA substrate, the protein of interest (800 nM Ded1p, 700 nM Mss116p, 2 μM Sub2p), and, where indicated, 0.5 mM ATP analogue (in equimolar mixture with $MgCl_2$) and incubated for 90 min at 19 °C. For RNA challenge reactions (Figure 1A), the RNA scavenger was added subsequently (1 μM final for Ded1p and Mss116p, 3 μM final for Sub2p) and incubated for 1 min. For dilution challenge (Figure 1B), the reactions were diluted 250-fold with buffer identical to the reaction buffer but without nucleotides or RNA. Then RNA scavenger was added to the diluted sample and incubated for 1 min. For the EDTA challenge (Figure 1C), 10 mM EDTA and scavenger RNA were added to each sample and incubated for 1 min. After the 1 min challenge period, glycerol was added to 25% (v/v), and the samples were applied to 7% nondenaturing PAGE gels. Protein−RNA complexes and single-stranded RNA were separated at 4 °C. Gels were dried, and the radiolabeled RNAs were visualized and quantified with a PhosphorImager and the ImageQuant 5.2 software (Molecular Dynamics).

To determine dissociation rate constants, binding reactions were assembled and incubated as described above, except that challenge times were varied in order to record dissociation time courses. Protein−RNA complexes and single-stranded RNA were separated at 4 °C on 7% nondenaturing gels, gels were dried, and the radiolabeled RNAs were visualized and quantified with a Phosphor Imager and ImageQuant 5.2 (Molecular Dynamics). Dissociation time courses were constructed by plotting the fraction bound RNA vs time. Dissociation rate constants were calculated by fitting the data sets to the integrated rate law of a homogeneous first-order reaction with an end point of zero.

To determine association rate constants, binding reactions were assembled as described above, except that the protein concentrations were varied. Subsequently, aliquots of 5 μL were removed at the respective time points. Binding was terminated by addition of scavenger RNA and glycerol (25% (v/v) final). Samples were then applied to 7% nondenaturing PAGE, and protein−RNA complexes and single-stranded RNA were separated, gels were dried, and the radiolabeled RNAs were visualized and quantified with a Phosphor Imager and Image Quant 5.2 (Molecular Dynamics). Time courses were constructed by plotting the fraction bound RNA vs time and observed (pseudo-first-order) association rate constants were obtained by fitting the data sets to the integrated rate law of a homogeneous first-order reaction. Second-order association rate constants were calculated by determining observed association rate constants at several protein concentrations, plotting these rate constants vs protein concentrations, and fitting the resulting data set to a linear equation. The slope equals the second-order association rate constant.

**ATP Hydrolysis Reactions.** ATPase measurements were performed at 19 °C in 20 μL of a buffer containing 40 mMTris·HCl (pH 8.0), 50 mM NaCl, 0.5 mM $MgCl_2$, 2 mM DTT, 0.6 unit·μL$^{-1}$ RNasin, 0.01% (v/v) IGEPAL, and 0.4 μM Ded1p. Ded1p was preincubated with or without 0.5 mM nucleotide analogue and 2 μM RNA (16 nt) for 90 min before reaction start. Reactions were initiated by addition of a mixture of trace amounts of [$\gamma$-$^{32}$P] ATP and 0.5 mM ATP. If the nucleotide analogue and RNA were not preincubated, they were added with the initiation of the reaction. All reactions contained equimolar nucleotide and $MgCl_2$ with 0.5 mM $MgCl_2$ excess. At various time points, 1 μL aliquots were removed and applied to a PEI-cellulose thin-layer chromatography plate (20 cm × 20 cm; Selecto Scientific). The PEI plate was developed with 1.5 M LiCl and 2 M formic acid and subsequently dried. Radioactivity was quantified with a PhosphorImager (GE) and the ImageQuant software (Mol. Dynamics). Initial rates of ATP hydrolysis ($v_0$) were determined by linear least-squares fit to the initial phase of the reaction (fraction ATP hydrolyzed ≤ 0.15).

**Unwinding Reactions.** Duplex unwinding was measured as described.[15] Prior to the reactions, RNA was incubated with enzyme for 5 min. Unwinding reactions (19 °C) were initiated by adding equimolar ATP or analogue and $MgCl_2$. Reactions were quenched with 5 vol of stop buffer (50 mM EDTA, 1% SDS, 0.01% bromophenol blue, 0.01% xylene cyanol, 10% (v/v) glycerol). Aliquots were applied to 15% nondenaturing polyacrylamide gel. Duplex and single-stranded RNA were separated at room temperature at 10 V·cm$^{-1}$. Gels were dried and the radiolabeled RNAs were visualized with a PhosphorImager and ImageQuant software 5.2 (Molecular Dynamics).

**Single-Molecule FRET Measurements.** Single-molecule FRET was measured in a home-built, total internal reflection (TIR) microscope setup, analogous to the system described by Zhuang et al.[20] (Nikon TE300 microscope, Pentamax Gen III CCD, Princeton Instruments, 50 mW, frequency doubled solid-state laser, Crystalaser). RNA samples (50 pM, fluorescently labeled and biotinylated duplex) were immobilized in a flow-cell, coated with polyethylene glycol (PEG) to prevent nonspecific protein absorption. The PEG coating was

accomplished by covalently attaching a mixture of PEG-NHS (3000−5000 Da) and biotinylated PEG-NHS (3000 Da) (Shearwater) to flow-cells that were amino-functionalized with Vectabond (Vector).[21] Biotinylated RNA samples were immobilized by binding to streptavidin (Molecular Probes) bound to the biotinylated PEG. Nonspecific binding of the labeled RNA complex (tested by omission of streptavidin) was less than 5% of the specific binding. Photobleaching studies confirmed that more than 90% of the fluorescent spots corresponded to single fluorophores.

Binding reactions were conducted in the buffer used for the above binding experiments, except that 5% (v/v) glucose was added together with an oxygen-scavenging system containing glucose oxidase (Sigma) and catalase (Sigma).[22] Experiments involving wash steps employed a wash buffer identical to the binding buffer, but without ADP, fluoride salts, and $Mg^{2+}$.

Samples were excited by TIR (532 nm), and the fluorescence was collected through a 60×, 1.2 N.A. water immersion objective (Nikon). Excitation light was blocked with a 550 nm long-path filter (Omega). Donor and acceptor fluorescence images were split by a dichroic filter (650 nm, Omega). The two resulting images were projected onto one-half of the CCD. Over 10 min multiple single-molecule time traces of about 20−30 s length were collected at a rate of 10 frames per second (fps), using customized software. Fluorescence and corresponding FRET values were computed as described.[22] SmFRET histograms (Figure 2B) were obtained by plotting the FRET values of individual complexes averaged over five frames. Histograms were fit with a Gaussian function to obtain the reported smFRET value.

## RESULTS

**Ded1p Forms Stable Complexes with RNA and the ATP Ground-State Analogue ADP-BeF$_x$.** To analyze complexes formed between RNA and DEAD-box helicases at defined stages of the ATP hydrolysis cycle, we first examined Ded1p bound to RNA in the presence of the nonhydrolyzable ground-state ATP analogue ADP-BeF$_x$. Ded1p is a prototypical DEAD-box helicase from *Saccharomyces cerevisiae*.[23] The enzyme is involved in translation initiation and possibly in pre-mRNA splicing and RNA export.[8,24] RNA helicase, strand annealing, and protein displacement activities of Ded1p have been characterized *in vitro*.[15,23,25,26] The ATP ground-state analogue ADP-BeF$_x$ was chosen, based on its structure in DEAD-box and other RNA helicases.[27−29] ADP-BeF$_x$ promotes RNA duplex unwinding for several DEAD-box helicases.[19,30] We used a gel electrophoretic mobility shift assay (EMSA) to analyze binding of a 10 nt single-stranded RNA to Ded1p in the presence of ADP-BeF$_x$ (Figure 1). The 10 nt RNA was the shortest oligonucleotide bound stably by Ded1p with all ATP analogues used in the present study (data not shown). A 10 nt RNA is also bound by the DEAD-box helicase Mss116p in crystal structures.[28] Without ADP-BeF$_x$, no stable Ded1p-RNA binding was seen (Figure 1A, lane 2).

To qualitatively assess dissociation of the 10 nt RNA from the RNA−Ded1p−ADP-BeF$_x$ complex, we challenged the completely formed complex with an excess of unlabeled scavenger RNA for 1 min (Figure 1A). The efficiency of the RNA challenge was verified by addition of scavenger RNA prior to Ded1p, which prevented Ded1p from binding to the 10 nt substrate RNA (Figure 1A, lane 4). With preformed RNA−Ded1p−ADP-BeF$_x$ complex, no significant release of labeled RNA was observed during the chase period (Figure 1A, lane 3).

We next tested whether ADP-BeF$_x$ dissociated from the Ded1p−RNA complex faster than the RNA. We monitored ADP-BeF$_x$ dissociation through dilution of preformed RNA−Ded1p−ADP-BeF$_x$ complex by a factor of 250 (Figure 1B). This dilution was sufficient to prevent *de novo* formation of Ded1p-RNA complex during the experiment (Figure 1B, lane 4). The amount of RNA−Ded1p−ADP-BeF$_x$ complex 1 min after dilution remained virtually unchanged from the amount of complex before dilution, indicating no significant dissociation of ADP-BeF$_x$ within 1 min (Figure 1B, lane 3).

We then examined dissociation of $Mg^{2+}$ from the RNA−Ded1p−ADP-BeF$_x$ complex. $Mg^{2+}$ is necessary for binding of ATP and ATP analogues to DEAD-box and other helicases.[31] To probe the dissociation of $Mg^{2+}$, we challenged preformed RNA−Ded1p−ADP-BeF$_x$ complex with excess EDTA, which binds free and dissociating $Mg^{2+}$ (Figure 1C). The preformed RNA−Ded1p−ADP-BeF$_x$ complex was resistant to the 1 min EDTA challenge (Figure 1C, lane 3). As expected, addition of EDTA during complex formation completely prevented complex assembly (Figure 1C, lane 4). Collectively, the challenge of preformed RNA−Ded1p−ADP-BeF$_x$ complex with scavenger RNA, dilution, and EDTA demonstrated that RNA, nucleotide, and $Mg^{2+}$ all dissociate with lifetimes exceeding minutes. These findings suggested a long-lived complex where little exchange of nucleotide and $Mg^{2+}$ occurs during the experiments.

To confirm and extend these observations, we tested whether the RNA−Ded1p−ADP-BeF$_x$ complex persisted after complete removal of all complex components in solution. To this end, we employed single molecule fluorescence resonance energy transfer (smFRET) and RNA substrates immobilized on a functionalized glass-surface in a flow cell (Figure 2A). This setup allowed the complete exchange of the reaction buffer after formation of RNA−Ded1p−ADP-BeF$_x$ complexes. Measurements were performed in a custom-made, total internal reflection detection setup (Materials and Methods). The fluorescently labeled RNA complex contained a duplex of 19 bp and a 25 nt ss region (Figure 2A). This substrate is unwound by Ded1p only exceedingly slowly with ADP-BeF$_x$ ($k_{unw} < 10^{-3}$ min$^{-1}$) and not at all in the presence of the other ATP analogues used here (data not shown). Therefore, unwinding did not influence the observations reported below.

SmFRET values for individual complexes were plotted in histograms (Figure 2B). Without Ded1p, the smFRET distribution showed a single peak at $E = 0.80$ and no significant changes in the distribution upon buffer exchange (Figure 2B, panels in row 1). Addition of BeF$_x$ did not affect the smFRET distribution in the absence of Ded1p (data not shown). Addition of Ded1p without nucleotide and with ADP alone caused a slight, yet reproducible shift in the peak of the smFRET distribution to $E = 0.83$. After buffer exchange, the peak in the smFRET distribution returned to the value seen without Ded1p (Figure 2B, row 2), most likely reflecting removal of dissociating Ded1p during buffer exchange. These observations are consistent with previously reported weak RNA binding by Ded1p in the absence of nucleotides.[23] The data further suggest that ADP alone does not induce stable Ded1p-RNA complexes, even though it promotes RNA binding by Ded1p.[32]

Binding of Ded1p to the RNA in the presence of ADP-BeF$_x$ complex resulted in a marked shift in the smFRET distribution (peak at $E = 0.35$), compared to the free RNA (Figure 2B, row 3). This shift in the smFRET distribution persisted after


dx.doi.org/10.1021/bi401540q | *Biochemistry* 2014, 53, 423−433

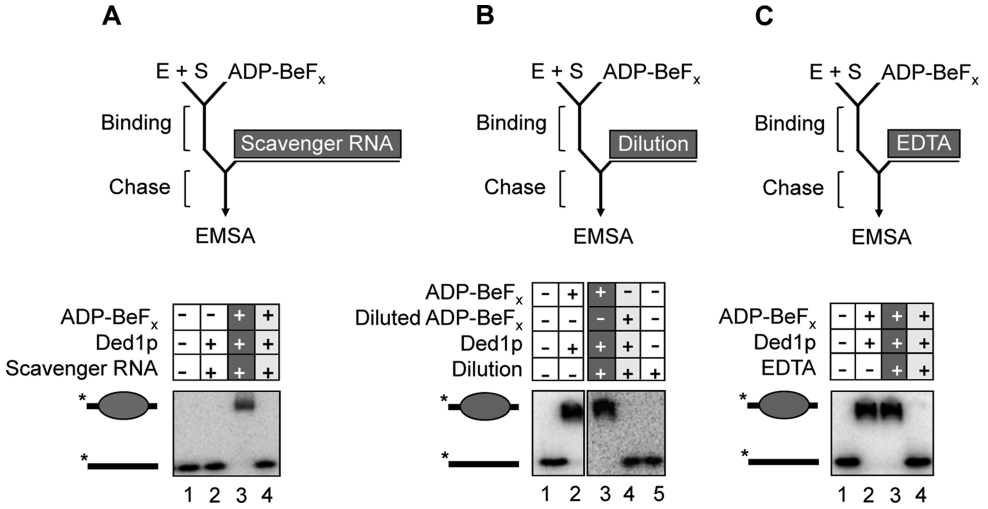


**Figure 1.** The Ded1p–RNA–ADP-BeF$_x$ complex is resistant to different challenge conditions. (A) Scheme for the binding reaction and subsequent challenge with scavenger RNA. Binding of Ded1p (800 nM final) to a radiolabeled, 10 nt RNA (0.5 nM final) in the presence of 0.5 mM ADP-BeF$_x$ was allowed to proceed for 90 min before incubation with scavenger RNA (73 nt, ssRNA, 1 $\mu$M final concentration) for 1 min, and subsequent application to nondenaturing PAGE. The lower panel is a representative PAGE scan of a binding reaction (lane 3) and controls, as indicated (lanes 1 and 2). Cartoons on the left indicate bound and free RNA, and asterisks mark the radiolabel. Lane 4: binding reaction where the scavenger RNA was added together with the radiolabeled substrate, to verify complete sequestration of Ded1p. (B) Scheme for the challenge by dilution. Binding reactions were performed as in panel (A), except that after 90 min incubation the samples were diluted by a factor of 250 and applied to PAGE after 1 min (lane 3). Lanes 1 and 2: RNA and a binding reaction before dilution. Lane 3: binding reaction. Lane 4: binding reaction (90 min) at concentrations established after the dilution, indicating no detectable binding of Ded1p to the RNA. (C) Scheme for the challenge with EDTA. Binding reactions were performed as in panel (A), except that after 90 min incubation, EDTA (10 mM final concentration) and scavenger RNA were added and incubated for 1 min, before PAGE loading (lane 3). Lanes 1 and 2: RNA and binding reaction before EDTA challenge. Lane 3: binding reaction. Lane 4: binding reaction where EDTA was added together with the radiolabeled substrate, to verify inability of Ded1p to bind the RNA in the presence of EDTA.

**Table 1. Dissociation and Association Rate Constants and Apparent Dissociation Constants for the Ded1p–RNA Complex with Different ATP Analogues**[a]

| | $k_{diss}$ (min$^{-1}$) | | | | |
|---|---|---|---|---|---|
| | RNA challenge | dilution | EDTA challenge | $k_{on}$ (min$^{-1}$ M$^{-1}$) | $K_{1/2}$ (M) |
| ADP-BeF$_x$ | (3.03 ± 0.18) × 10$^{-4}$ | (2.52 ± 0.15) × 10$^{-4}$ | (2.16 ± 0.13) × 10$^{-4}$ | (7.10 ± 0.93) × 10$^{6}$ | (4.27 ± 0.62) × 10$^{-11}$ |
| ADP-AlF$_x$ | (4.25 ± 0.25) × 10$^{-4}$ | (4.43 ± 0.22) × 10$^{-4}$ | (3.94 ± 0.15) × 10$^{-4}$ | (6.11 ± 0.56) × 10$^{4}$ | (6.96 ± 0.76) × 10$^{-9}$ |
| ADP-MgF$_x$ | (2.33 ± 0.18) × 10$^{-3}$ | (3.84 ± 0.23) × 10$^{-3}$ | (3.54 ± 0.21) × 10$^{-3}$ | (9.15 ± 0.91) × 10$^{2}$ | (2.55 ± 0.33) × 10$^{-6}$ |
| ADPNP | (5.65 ± 0.23) × 10$^{-3}$ | (6.04 ± 0.30) × 10$^{-3}$ | (6.11 ± 0.36) × 10$^{-3}$ | (1.64 ± 0.28) × 10$^{4}$ | (3.45 ± 0.60) × 10$^{-7}$ |

[a]Dissociation rate constants ($k_{diss}$) were determined from time courses monitoring the dissociation of Ded1p–RNA complexes with the various ATP analogues under RNA-, dilution-, and EDTA-challenge (Figure 1). Error ranges indicate the standard deviation of at least three independent measurements. Association rate constants ($k_{on}$) were determined from plots of apparent association rate constants at several Ded1p concentrations (see Methods). Error ranges indicate the standard error resulting from the fit of these plots. Time courses for the association of Ded1p–RNA complexes were measured at Ded1p concentrations from 50 nM to 800 nM in the presence of 0.5 mM ATP analogues. Apparent dissociation constants ($K_{1/2}$) were calculated according to $K_{1/2} = k_{diss}/k_{on}$.

complete buffer exchange, showing that the RNA–Ded1p–ADP-BeF$_x$ complex remained intact after removal of all complex components from the solution. This observation indicated no significant dissociation of any complex component at the time scale of the experiment (~10 min). This finding strongly supported the notion that the RNA–Ded1p–ADP-BeF$_x$ complex is long-lived and exists without exchange of nucleotide or $Mg^{2+}$ during the time scale of the experiments.

**Ded1p Forms Stable Complexes with RNA and the ATP Transition State Analogue ADP-AlF$_x$.** We next used smFRET to examine Ded1p–RNA complexes in the presence of the ATP transition state mimic ADP-AlF$_x$. This transition state mimic was chosen based on its structure in DEAD-box helicases.[10,28] ADP-AlF$_x$ does not promote unwinding by Ded1p.[19] Formation of the RNA–Ded1p–ADP-AlF$_x$ complex resulted in a significant shift in the smFRET distribution with a peak at $E$ = 0.35 (Figure 2B, row 4). This distribution was virtually identical to that seen with ADP-BeF$_x$. After buffer exchange, the smFRET distribution remained unchanged, again similar to observations with ADP-BeF$_x$. These results showed that the RNA–Ded1p–ADP-AlF$_x$ complex is also stable over the observation time and requires no exchange of nucleotide or $Mg^{2+}$.

We also analyzed Ded1p–RNA complexes formed with ADPNP, a widely used nonhydrolyzable ATP analogue that had previously been shown to promote RNA binding by Ded1p and other DEAD-box helicases.[23,30,33,34] However, it is not clear which, if any, defined stage of the ATP hydrolysis cycle is mimicked by ADPNP.[19,35–37] Formation of the Ded1p–RNA complex with ADPNP shifted the peak in the smFRET distribution to a value of $E$ = 0.40 (Figure 2B, row 4). This value was slightly, yet significantly, higher than the values


dx.doi.org/10.1021/bi401540q | Biochemistry 2014, 53, 423–433

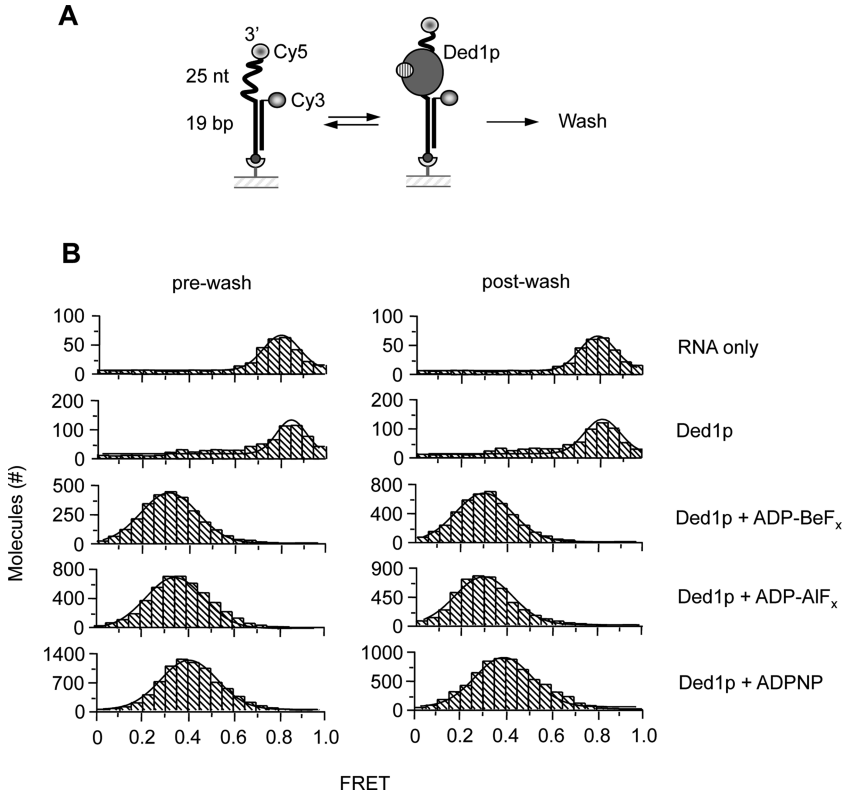


**Figure 2.** Ded1p−RNA complexes with various ATP analogues persist after complete removal of nucleotides and $Mg^{2+}$. (A) Schematics of the smFRET detection of the Ded1p−RNA complexes. Black lines represent RNA (19 bp, 25 nt ss region 3′ to the duplex, 2 nt ss region 5′ to the duplex that tethers the RNA via biotin-streptavidin to the glass surface of the flow-cell). For details on the smFRET measurements see Materials and Methods. The circles represent Cy5 and Cy3, as indicated. The RNA was immobilized; Ded1p and the various ATP analogues were added and incubated for 15 min. Subsequently, smFRET values of the reaction were measured and recorded as "prewash" values, as indicated. Then, the flow cell was purged with fresh reaction buffer without nucleotides. SmFRET values were measured and recorded as "postwash". (B) Histograms showing pre- and postwash smFRET values for RNA only (row 1) and Ded1p-RNA complexes without and with various ATP analogues, as indicated on the right.

observed with ADP-$BeF_x$ and ADP-$AlF_x$. After buffer exchange, the smFRET distribution with ADPNP remained unchanged, indicating no exchange of nucleotide or $Mg^{2+}$ from the complex with ADPNP during the experiment (Figure 2B, row 4). Notwithstanding the differences between the smFRET distributions with a ADPNP, compared to those with ADP-$BeF_x$ and ADP-$AlF_x$, the data for all three ATP analogues collectively indicate the existence of long-lived, nucleotide-dependent Ded1p−RNA complexes from which neither nucleotide nor $Mg^{2+}$ dissociate with a lifetime of $\tau_{diss}$ > 10 min.

**Formation of Stable Ded1p−RNA Complexes Requires Both, Nucleotide and RNA Binding.** Both ADP-$BeF_x$ and ADP-$AlF_x$ bind tightly to several ATPases and are often considered essentially irreversible inhibitors for these enzymes.[38,39] We therefore examined whether ADP-$BeF_x$ and ADP-$AlF_x$ bound to Ded1p in the absence of RNA. We rationalized that a persistent, stable complex of Ded1p with either ADP-$BeF_x$ or ADP-$AlF_x$ would inhibit RNA-dependent ATP hydrolysis of Ded1p. We thus measured the RNA-stimulated ATPase activity of Ded1p after preincubating Ded1p with or without nucleotide analogue in the absence and in the presence of RNA (Figure 3A,B). To detect robust ATPase activity, we used a substrate containing 16 bp and a 25 nt unpaired region.[32] The experiments could not be performed with $BeF_x$, since this compound strongly inhibited the ATPase reaction (data not shown), consistent with prior reports on other helicases.[40]

Addition of ADP, ADPNP, and ADP-$AlF_x$, without preincubation of analogue or RNA inhibited the ATPase activity of Ded1p by a factor of approximately 2 (Figure 3B). This degree of inhibition was similar to the level of inhibition with ADP (Figure 3B). This observation suggested that the inhibition seen with ADP-$AlF_x$ under these reaction conditions arose from ADP or from a nonstable binding of ADPNP but not from the formation of stable complex of Ded1p with either compound.

To assess the potency of ADP-fluoride compounds in general, we also added a reaction with ADP-NaF, which forms ADP-$MgF_x$ in the active site of ATPases. ADP-$MgF_x$ had been observed in crystal structures of the superfamily 1 helicase UvrD.[41] ADP-$MgF_x$ did not inhibit to a larger extent than ADP alone (Figure 3B). $AlF_x$ and $MgF_x$ without ADP did not inhibit the ATPase activity, indicating strict requirement of the nucleotide for the effect. Collectively, the data suggested that ADPNP, ADP-$AlF_x$, and ADP-$MgF_x$ did not form stable complexes with Ded1p in the absence of RNA.

We then preincubated Ded1p with RNA and the respective ATP analogues prior to addition of ATP (Figure 3C,D). Under these conditions, we observed strong inhibition of the ATPase activity by ADPNP, ADP-$AlF_x$, and ADP-$MgF_x$ (Figure 3D). These observations indicated that the formation of the stable Ded1p−RNA−ATP-analogue complex requires all three components. Notably, ADP-$MgF_x$ also appeared to form a stable complex with Ded1p and RNA, consistent with crystal


dx.doi.org/10.1021/bi401540q | *Biochemistry* 2014, 53, 423−433

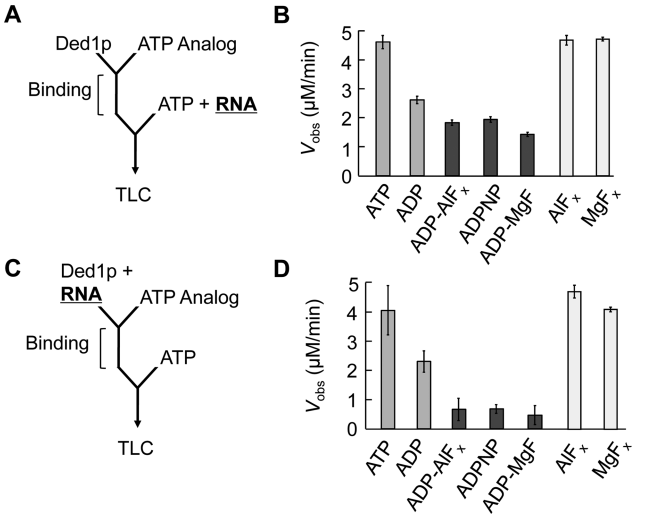


**Figure 3.** Formation of persistent Ded1p−RNA complexes requires both nucleotide and RNA binding. (A) Schematics for the reaction of Ded1p with ATP analogue without preincubation. 0.4 $\mu$M Ded1p was incubated for 90 min with 0.5 mM ATP analogue, or ADP. ATPase reactions were initiated with ATP (0.5 mM final) and RNA (2 $\mu$M final, 16 bp, 25 nt ss region 3′ to the duplex). All reactions contained equimolar nucleotide and $MgCl_2$ with additional 0.5 mM excess of $MgCl_2$. (B) Initial reaction rates $v_{obs}$ for each ATP analogue and for controls with $AlF_x$ and $MgF_x$. Errors show the standard deviation of at least three independent experiments. (C) Schematics for the reaction with preincubation of Ded1p with ATP analogue and RNA before initiation of ATPase assay. Concentrations were as above; preincubation was for 90 min. ATPase reactions were initiated with ATP (0.5 mM final). (D) Initial reaction rates $v_{obs}$ for each ATP analogue. Errors show the standard deviation of at least three independent experiments.

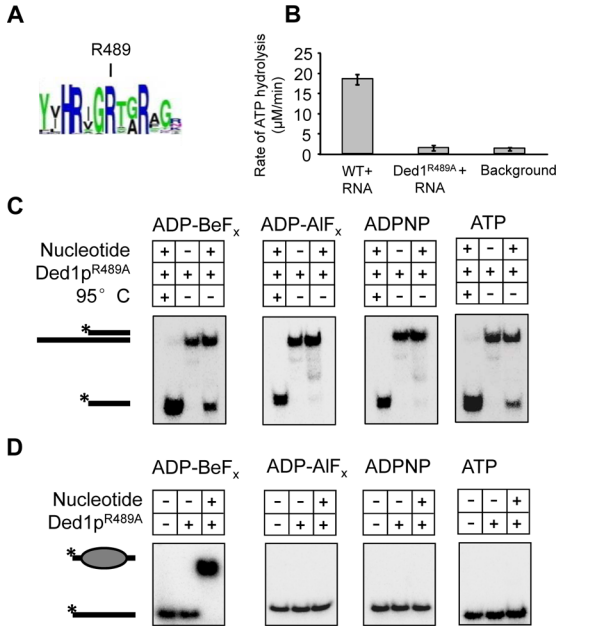


**Figure 4.** $Ded1p^{R498A}$ forms persistent RNA complexes with ADP-BeFx but not with ADP-$AlF_x$. (A) Sequence conservation in motif VI of DEAD-box helicases.[53] (B) RNA-stimulated ATPase activity of $Ded1p^{R498A}$. Plotted are $v_{obs}$ for 1 $\mu$M protein, 2 $\mu$M RNA substrate (16-bp with 3′ 25-nt unpaired RNA), and 1 mM ATP. Bk indicates background ATP hydrolysis in a reaction without protein. (C) Unwinding reactions (60 min) with 0.1 nM RNA substrate (10-bp with 3′ 25-nt unpaired RNA), 1 $\mu$M $Ded1p^{R489A}$ with 0.5 mM ATP or analogue (0.5 mM ADP for ADP-$BeF_x$ and ADP-$AlF_x$). Cartoons indicate the RNA species; asterisks mark the radiolabel. (D) Binding of 1 $\mu$M Ded1p-R489A to 0.1 nM 25-nt single-stranded RNA in the absence or presence of 0.5 mM ATP or analogue (0.5 mM ADP for ADP-BeFx and ADP-$AlF_x$). Components were incubated for 60 min. Before application to PAGE, excess single-stranded RNA (1 $\mu$M final, 73 nt scavenger RNA) was added and incubated for 1 min to bind free Ded1p. Cartoons indicate bound and free RNA, the asterisk marks the radiolabel.

structures of the related helicase UvrD.[41] With ADP alone, the degree of inhibition did not exceed the inhibition seen with addition of ADP prior to the RNA addition. This result supports the notion that the inhibition seen with the analogues incubated with Ded1p alone was due to ADP (Figure 3A,B). Again, no inhibition was observed by $AlF_x$ or $MgF_x$ without ADP (Figure 3D).

**Ded1p-RNA Complexes with ADP-$BeF_x$ and ADP-$AlF_x$ Have Lifetimes of Many Hours.** Having shown that the stable complexes required both RNA and the ATP analogue, we next assessed the persistence the complexes in a quantitative fashion. To this end, we measured dissociation and association rate constants of the complexes, using the gel-based approach described in Figure 1. Dissociation rate constants were determined with RNA-, dilution-, and EDTA-challenge, measuring the RNA release over time (Table 1). In the presence of ADP-$BeF_x$, the Ded1p−RNA complex dissociated with rate constants between $k_{diss} = (3.03 \pm 0.18) \times 10^{-4}$ $min^{-1}$ (RNA challenge) and $k_{diss} = (2.16 \pm 0.15) \times 10^{-4}$ $min^{-1}$ (EDTA challenge) (Table 1). These dissociation rate constants translate into a half-life between $t_{1/2} \approx 38$ h (RNA challenge) and $t_{1/2} \approx 53$ h (EDTA challenge), consistent with the virtually unchanged persistence of the complex during the time frame of the qualitative challenge experiments and the smFRET measurements (Figures 1 and 2). Although differences between measured dissociation rate constants with varying challenge methods slightly exceed the respective error ranges, we believe that these variations are probably not functionally significant. The relative insensitivity of the dissociation rate constants to the different challenge conditions indicates that nucleotide and $Mg^{2+}$ are bound as long as RNA in the complex. This finding suggests cooperative disassembly of the complex; that is, the entire complex disintegrates quickly if any of the components (RNA, nucleotide, $Mg^{2+}$) dissociates. This notion is consistent with the requirement for RNA, nucleotide, and Ded1p to form stable complexes, shown above (Figure 3).

We next measured the association rate constant ($k_{on}$), for the binding of ADP-$BeF_x$ to the Ded1p−RNA complex. This rate constant was several orders lower than the diffusion limit (Table 1). This observation suggests, perhaps not unexpectedly, that formation of the long-lived Ded1p−RNA−ADP-$BeF_x$ complex involves one or more conformational changes. The computed thermodynamic stability of the complex ($K_{1/2}$) was in the picomolar range (Table 1).

Dissociation rate constants of the Ded1p−RNA complex with ADP-$AlF_x$ were similar to those with ADP-$BeF_x$ (Table 1). Different challenge methods impacted the dissociation rate constants only slightly. Thus, as seen with ADP-$BeF_x$, none of the complex components dissociates faster than other components from the complex formed with ADP-$AlF_x$ . However, the association rate constant with ADP-$AlF_x$ was 2 orders of magnitude lower than with ADP-$BeF_x$ (Table 1). This result suggests that the transition-state mimic ADP-$AlF_x$ was


dx.doi.org/10.1021/bi401540q | Biochemistry 2014, 53, 423−433

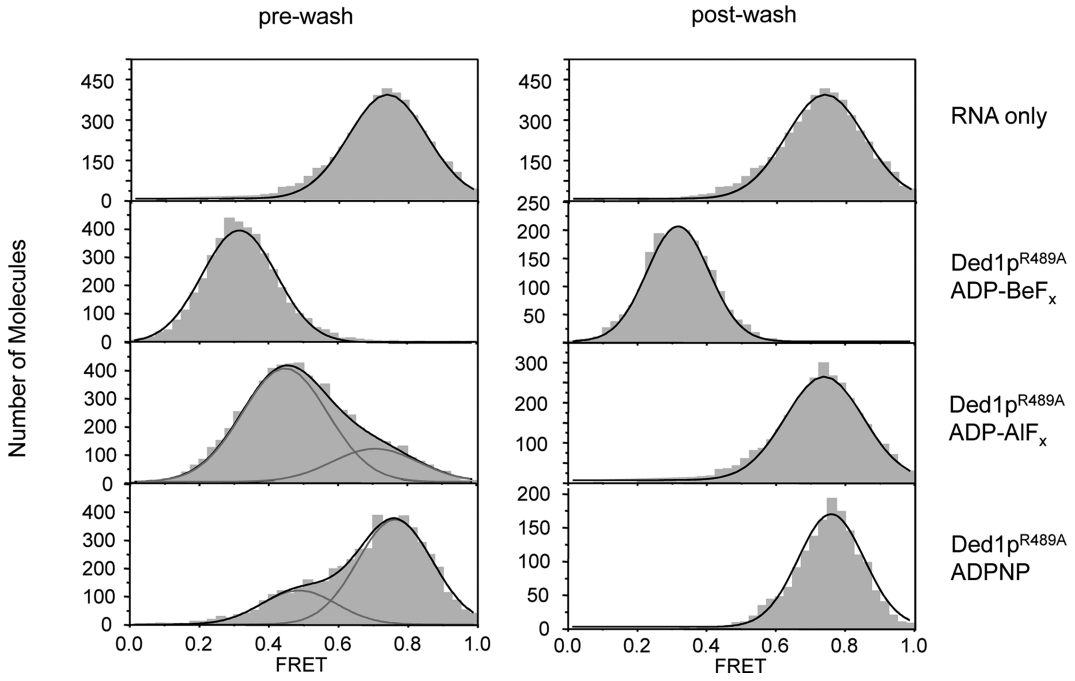


**Figure 5.** Response of Ded1p$^{R489A}$-RNA complexes with ATP analogues to buffer exchange. SmFRET setup, RNA substrate, and reaction conditions were as described in Figure 2. Ded1p$^{R489A}$ was at 1 $\mu$M in the binding reactions, ATP analogues as described in Figure 2. Left panels: smFRET values for Ded1p$^{R489A}$–RNA complexes with indicated ATP analogues before buffer exchange. Distributions with RNA only and ADP-BeF$_x$ were fit to a single Gaussian (black lines). Distributions with ADP-AlF$_x$ and ADPNP were fit to two Gaussians (light gray lines), and the sum of the two distributions is indicated by the black line. Right panels: smFRET values for Ded1p$^{R489A}$–RNA complexes with indicated ATP analogues after buffer exchange. All distributions were fit to a single Gaussian (black lines).

not as readily accommodated into the long-lived complex as the ground-state analogue ADP-BeF$_x$. As a consequence, the stability ($K_{1/2}$) of the complex with ADP-AlF$_x$, although in the nanomolar range, was lower than with ADP-BeF$_x$ (Table 1).

We then examined whether long-lived Ded1p–RNA complexes could be formed with just ADP-MgF$_x$. A relatively long-lived Ded1p–RNA complex did form, but dissociation rate constants were an order of magnitude higher than with ADP-AlF$_x$ and ADP-BeF$_x$ (Table 1). Again, different challenge methods did not have large effects on the dissociation rate constants. However, the complex with ADP-MgF$_x$ formed exceedingly slowly. The association rate constant was about 4 orders of magnitude lower than with ADP-BeF$_x$ (Table 1). Consequently, the thermodynamic stability of the complex ($K_{1/2}$) was only in the micromolar range, 5 orders of magnitude lower than with ADP-BeF$_x$ (Table 1).

With ADPNP, dissociation rate constants of the Ded1p–RNA complex were closer to values with ADP-MgF$_x$ than to those with ADP-BeF$_x$ and ADP-AlF$_x$ (Table 1) As seen with the other ATP analogues, the challenge method did not have large effects on the lifetimes of the complexes (Table 1). The association rate constant with ADPNP was similar to that seen with ADP-AlF$_x$, revealing that ADPNP, like ADP-AlF$_x$ was not as readily accommodated in the active site as the ground state analogue ADP-BeF$_x$. The thermodynamic stability of the complex with ADPNP was also notably lower than the stabilities of the complexes formed with both ADP-BeF$_x$ and ADP-AlF$_x$, but higher than with ADP-MgF$_x$ (Table 1).

Taken together, the dissociation and association rate constants of Ded1p-RNA complexes with the various ATP analogues revealed remarkably long-lived complexes. The data also show that neither nucleotide nor $Mg^{2+}$ dissociates more rapidly than the RNA from the complexes.

**Mutation of the Arginine Finger in Ded1p Eliminates Formation of Stable Complexes with the Transition State Analogue.** The similar dissociation rate constants of Ded1p–RNA complexes with both ADP-BeF$_x$ and ADP-AlF$_x$ prompted us to examine the notion that the two analogues indeed represented functional mimics for distinct stages of the ATP hydrolysis cycle. To this end, we mutated in Ded1p the arginine "finger" (R489), which is conserved in all SF2 helicases and located in helicase motif VI (Figure 4A). In the cell, this Ded1p mutation is lethal.[24] The arginine "finger" has been implied in stabilizing the transition state of the ATP hydrolysis reaction in helicases.[31] We reasoned that mutation of this amino acid should allow formation of a stable Ded1p–RNA complex with the ground-state ATP analogue, but not with the transition state analogue.

As expected, the R489A mutation virtually eliminated the RNA-stimulated ATPase activity of Ded1p (Figure 4B). ATPase activity of Ded1p$^{R489A}$ was reduced to background levels of wt Ded1p without added RNA (Figure 4B). To assess the functional integrity of Ded1p$^{R489A}$, we tested strand displacement with ATP analogues (Figure 4C). We had previously shown that ADP-BeF$_x$ promotes duplex unwinding by wtDed1p.[19] We observed clear strand separation with ADP-BeF$_x$, but not with the other analogues, confirming basic functional integrity for Ded1p$^{R489A}$ (Figure 4C). Nonetheless, the rate constant for strand separation was slower by a factor of 173, compared to wtDed1p (data not shown). This result suggests that ATP binding, not only stabilization of the transition state, might be impacted by the mutation.

As expected, unwinding by Ded1p$^{R489A}$ was also observed with ATP (Figure 4C), given that ATP binding promotes


dx.doi.org/10.1021/bi401540q | *Biochemistry* 2014, 53, 423–433

strand separation by Ded1p.[19] The unwinding rate constant with ATP was again lower than with wtDed1p (data not shown), consistent with the notion that the mutation also affects ATP binding. Despite the potential impact of the R489A mutation on ATP binding, Ded1p$^{R489A}$ formed a stable complex RNA with ADP-BeF$_x$ (Figure 4D). However, no stable complex formation was seen with ADP-AlF$_x$ and ADPNP (Figure 4D). This pattern contrasts with wtDed1p (Figure 2) and is therefore consistent with the expectation that Ded1p$^{R489A}$ accommodates the ATP ground state analogue, but not the transition-state analogue. The data thus suggested that ADP-BeF$_x$ and ADP-AlF$_x$ indeed represented functional mimics for different stages of the ATP hydrolysis cycle. ATP could not induce stable RNA binding by Ded1p$^{R489A}$ (Figure 4D). This result is consistent with the notion that Ded1p$^{R489A}$ retains residual ATPase activity that suffices to destabilize the complexes. However, such residual activity is clearly not enough to stabilize the transition state to levels comparable to wtDed1p.

The stable RNA−Ded1p$^{R489A}$−ADP-BeF$_x$ complex also persisted after complete removal of all complex components in solution, as measured by smFRET (Figure 5). We observed a shift in the smFRET distribution with ADP-BeF$_x$ that remained after buffer exchange (Figure 5). With ADP-AlF$_x$ the distribution shifted before washing but the shift did not persist after the wash (Figure 5). Notably, the shift before the wash differed from the shift seen with ADP-BeF$_x$, indicating differences between the complexes with both analogues. Similarly, ADPNP did not induce a shift that persisted after the wash (Figure 5). Collectively, the results obtained with Ded1p$^{R489A}$ showed that mutation of the arginine finger allowed only the ATP ground state analogue to induce long-lived complexes, but not the transition state analogue. The data provide evidence that ADP-BeF$_x$ is functionally distinct from ADP-AlF, and we can conclude that wtDed1p is able to form long-lived complexes with RNA in both ATP ground and transition state.

**The DEAD-Box Helicases Mss116p and Sub2p also Form Long-Lived RNA Complexes with ADP-BeF$_x$, but Only Mss116p Forms Such Complexes with ADP-AlF$_x$.** Our findings with Ded1p raised the question whether other DEAD-box helicases also formed comparably long-lived, nucleotide-dependent complexes with RNA. We therefore measured dissociation rate constants for nucleotide-dependent complexes with two other DEAD-box helicases and RNA. First, we determined dissociation rate constants for the complexes formed by Mss116p, another DEAD-box protein from *S. cerevisiae*.[16,42] Like Ded1p, Mss116p unwinds RNA with ADP-BeF$_x$, but not with ADP-AlF$_x$ or ADPNP.[19] Mss116p formed complexes with the 10 nt RNA in the presence of ADP-BeF$_x$ (Figure 6A,B). The dissociation rate constants for the complex with ADP-BeF$_x$ were roughly 1 order of magnitude higher than for Ded1p but still indicative of long-lived complexes ($t_{1/2} \approx 6.7$ h, Figure 6B). Dissociation rate constants with ADP-AlF$_x$, ADP-MgF$_x$, and ADPNP were slightly higher than with ADP-BeF$_x$ but in a similar range (Figure 6B). Challenge with EDTA did not lead to large changes in the dissociation rate constants, indicating that $Mg^{2+}$ and nucleotide did not dissociate more rapidly than the RNA from the complex. These observations show that Mss116p, like Ded1p, forms long-lived, nucleotide-dependent RNA complexes from which neither nucleotide nor $Mg^{2+}$ dissociate. Nonetheless, subtle differences exist between the complexes formed by Ded1p and Mss116p. While the

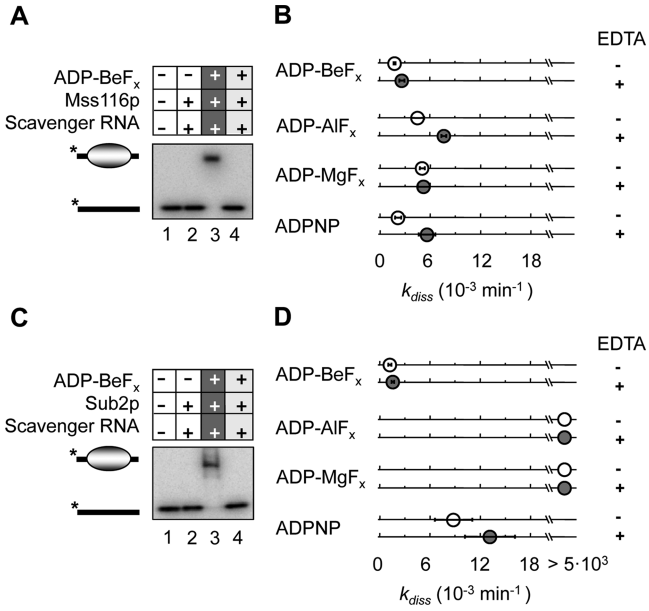


**Figure 6.** Mss116p and Sub2p form long-lived complexes with RNA and various ATP analogues. (A) Binding reactions (90 min) of 700 nM Mss116p to 0.5 nM 10-nt ssRNA with 0.5 mM ADP-BeF$_x$ after challenge with scavenger RNA. Reactions were performed as outlined in Figure 1A, and substrate and scavenger RNAs were identical to those in Figure 1A. The representative PAGE scan shows the binding reaction (lane 3) and controls, as indicated (lanes 1 and 2). Lane 4 shows a binding reaction where the scavenger RNA was added together with the radio-labeled substrate, to verify complete "scavenging" of Mss116p. Cartoons on the left indicate bound and free RNA, asterisks mark the radiolabel. (B) Dissociation rate constants for Mss116p-RNA complexes with the ATP analogues indicated, measured under RNA and EDTA challenge conditions. The plus indicates the EDTA challenge. Dissociation rate constants were measured as in Table 1. (C) Binding reactions (90 min) of 2 $\mu$M Sub2p to 0.5 nM 10-nt ssRNA with 0.5 mM ADP-BeF$_x$ after challenge with scavenger RNA. Reactions were performed as outlined in Figure 1A, and substrate and scavenger RNAs were identical to those in Figure 1A (lanes as in Figure 3A). (D) Dissociation rate constants for Sub2p-RNA complexes with the ATP analogues indicated, measured under RNA and EDTA challenge conditions. The plus sign indicates the EDTA challenge. Dissociation rate constants were measured as described in Table 1.

RNA−Ded1p complexes with ADP-BeF$_x$ and ADP-AlF$_x$ had notably longer half-lives than the complexes with ADP-MgF$_x$ and ADPNP, these differences were much smaller for Mss116p, possibly correlating with the virtually identical crystal structures of these complexes.[28]

We extended our investigation to the DEAD-box protein Sub2p from *S. cerevisiae*.[43,44] Sub2p is a *bona fide* DEAD-box helicase, despite a slightly divergent D-E-C-D sequence in the helicase motif II.[45] Available structural information for Sub2p's human ortholog UAP56, whose motif II also reads D-E-C-D, indicates no structural differences in this region, compared to other DEAD-box proteins.[46,47] Like other DEAD-box helicases, Sub2p unwinds RNA duplexes with ADP-BeF$_x$, but not with ADP-AlF$_x$ or ADPNP (data not shown).

Sub2p formed stable complexes with RNA and ADP-BeF$_x$ (Figure 6C), as seen for Ded1p and Mss116p. Dissociation rate constants for the Sub2p-RNA complex with ADP-BeF$_x$ corresponded to a half-lives of $t_{1/2} \approx 15$ h (Figure 6D), and challenge with EDTA did not significantly alter the dissociation rate constant. In marked contrast to Mss116p and Ded1p,


dx.doi.org/10.1021/bi401540q | *Biochemistry* 2014, 53, 423−433

Sub2p did not form stable RNA complexes with ADP-AlF$_x$ or ADP-MgF$_x$ (Figure 6D), although it is possible that formation of the complexes is extremely slow. However, we did not detect complex even after 4 h of incubation (data not shown). This observation marks an upper limit for the binding rate constant of roughly $k_{on} < 100\ M^{-1}\ min^{-1}$, a value several orders of magnitude lower than binding rate constants seen for Ded1p (Table 1). Sub2p formed a persistent complex with RNA in the presence of ADPNP, ($t_{1/2} \approx 1$ h, Figure 6D), but the dissociation rate constant was notably higher than with ADP-BeF$_x$. The dissociation rate constant with ADPNP did not significantly change upon EDTA challenge (Figure 6D).

The observations with Mss116p and Sub2p show that these two RNA helicases, like Ded1p, form long-lived RNA complexes with the ATP ground state analogue. The inability of Sub2p to form comparable complexes with the transition state analogue suggests that different stages of the ATP hydrolysis differentially modulate RNA binding in distinct DEAD-box helicases.

## DISCUSSION

In this study, we provide the first direct demonstration that DEAD-box helicases can form nucleotide-dependent, extraordinarily long-lived complexes with RNA. Our data indicate that a subset, and perhaps all DEAD-box helicases, have an inherent capacity to function as potent, ATP-dependent RNA clamps. Although RNA clamping in a physiological setting would require other factors to arrest the ATP hydrolysis cycle at appropriate times, similar to the scenario seen with eIF4A-III in the EJC,[10−12] our findings show that such factors are not needed for persistent RNA binding of the DEAD-box helicase. The ability to clamp to RNA in an ATP-dependent fashion resides in the helicase itself.

We found that the three tested helicases, Ded1p, Mss116p, and Sub2p, all form long-lived RNA complexes in the presence of the nonhydrolyzable ATP ground-state analogue, ADP-BeF$_x$. Ded1p and Mss116p also form comparably long-lived RNA complexes with the ATP transition-state analogue ADP-AlF$_x$, but Sub2p does not. These data suggest that different states of the ATP hydrolysis cycle do not necessarily modulate RNA binding in the same way for all DEAD-box helicases. This notion parallels recent findings showing that effects of ADP and ATP on RNA affinity also differ for distinct DEAD-box helicases.[3,32] Alternatively, the ATP transition state might differ for distinct DEAD-box helicases, and ADP-AlF$_x$ might not represent as good a transition-state analogue for Sub2p as for Ded1p and Mss116p. A structural basis for any of these possible differences is not apparent from available crystal structures.

Formation of nucleotide-dependent, long-lived complexes has been seen for other, non-DEAD-box helicases with RNA or DNA, but there are important differences. For example, the SF1 DNA helicase Rep and the viral SF2 RNA helicase NPH-II form long-lived complexes only in the presence of ADP-AlF$_x$.[48,49] However, both of these helicases translocate processively along DNA or RNA in an ATP-dependent fashion.[17,50] A persistent complex with the ATP ground state could potentially interfer with this movement and is thus unlikely to occur during unwinding, although this cannot be ruled out categorically. The transition state, on the other hand, is transient by definition, and more unlikely to impede movement.

DEAD-box helicases do not translocate and unwinding involves an RNA binding step coupled to an ATP-induced conformational change.[3] We speculate that the coupling of the ATP ground state to long-lived RNA binding might favor clamping more than a tight complex in the transition state. It might be more suitable for other proteins to arrest the tightly bound complex in the ATP ground state and turn the helicase into an RNA clamp as proposed for the EJC.[10]

Our data directly show that persistent DEAD-box helicase−RNA−nucleotide complexes require all three components (Figure 3). Without RNA, the helicases do not bind ADP-BeFx or ADP-AlFx comparably tight (Figure 3). In this sense, DEAD-box helicases differ from the cytoskeletal motors kinesin and myosin (S1), which form long-lived proteins complexes with ADP-BeF$_x$ and ADP-AlF$_x$, while the lattices (microtubuli and actin, respectively) destabilize the protein-nucleotide complexes.[39] In sum, our data suggest that the long-lived nucleotide-dependent RNA complexes with DEAD-box helicases differ in significant aspects from long-lived complexes seen with other ATPases and ADP-BeF$_x$ or ADP-AlF$_x$, or both. We speculate that the properties of the DEAD-box helicase complexes are particularly conducive to RNA clamping.

The remarkably long lifetimes of the nucleotide−RNA−protein complexes and the inability of nucleotide and $Mg^{2+}$ to dissociate at a faster rate provide functional context for recent structures of DEAD-box helicases with RNA and ATP analogues.[28,29] In these structures, the water molecules involved in nucleotide and $Mg^{2+}$ binding are isolated from bulk water.[10,28] Similar exclusion of excess water is seen in other NTP-dependent enzymes as well, perhaps to avoid unregulated NTP hydrolysis.[51] The long lifetime of the complexes seen in our present study, combined with the lack of $Mg^{2+}$ exchange may functionally reflect this "sealing" of the nucleotide and phosphate binding sites against bulk water. In addition, the long lifetimes and the lack of $Mg^{2+}$ and nucleotide exchange for both ground and transition state analogues suggest that both states can be accommodated in an essentially sealed ATP binding site. This scenario is consistent with data for eIF4A-III in the EJC, showing reversible hydrolysis and suggesting multiple interconversions between ATP ground state and hydrolyzed ADP-P$_i$.[10] Our data extend these observations by showing long-lived, nucleotide-dependent Ded1p-RNA complexes without other protein cofactors.

We note that it remains formally possible that nucleotide or $Mg^{2+}$, or both, dissociate more rapidly than indicated by the dissociation rate constant, but that Ded1p remains stably bound to the RNA without the nucleotide or $Mg^{2+}$ until the RNA dissociates. In principle, such molecular memory could explain how nucleotide or $Mg^{2+}$ dissociate faster than the RNA, but without apparent change in the dissociation rate constant for the RNA. However, the measured dissociation constants would imply molecular memory over many hours. This time frame, to our knowledge, exceeds molecular memory effects in proteins by many orders of magnitude.[52] We therefore favor the more straightforward interpretation of our observations: persistent binding of the nucleotide and $Mg^{2+}$ in the complex and cooperative complex disassembly.

Finally, our smFRET data suggest differences in RNA−protein complexes formed with ADPNP versus those with ADP-BeF$_x$ or ADP-AlF$_x$ (Figure 2). ADPNP has been previously shown to not clearly correspond a state in the ATP-hydrolysis cycle for DEAD-box proteins,[14] even though the crystal structures of the DEAD-box protein Mss116p bound to a 10 nt RNA with ADPNP were essentially identical to those with ADP-BeF$_x$ and ADP-AlF$_x$.[28] We see a shift of the smFRET

peak of Ded1p bound to RNA with ADPNP compared to peaks seen with ADP-$BeF_x$ and ADP-$AlF_x$ (Figure 2), suggesting that these two ATP analogues induce conformations of the Ded1p–RNA complex that differ from those with ADPNP. These differences however could be caused by small structural changes that may not be reflected in the crystal structures of the complexes. It is also possible that ADPNP induces slightly different conformations in the RNA complexes of Ded1p and Mss116p.

## AUTHOR INFORMATION


### Corresponding Author

*E-mail: exj13@case.edu. Phone: (216) 368-3336. Fax: (216) 368-3419.



### Funding

Funding is from NIH (GM067700 to E.J.).


### Notes

The authors declare no competing financial interest.

## ACKNOWLEDGMENTS

We thank the members of the Jankowsky lab for helpful discussions. Purified Mss116p was a gift from Drs. Alan Lambowitz and Mark del Campo (UT Austin). Purified Sub2p was a gift from Drs. Ditlev Broderson, Torben Heick-Jensen, and Andreas Boggild (University of Aarhus, Denmark).

## REFERENCES


(1) Linder, P., and Jankowsky, E. (2011) From unwinding to clamping - the DEAD box RNA helicase family. *Nat. Rev. Mol. Cell Biol. 12*, 505–516.

(2) Jankowsky, E. (2010) RNA helicases at work: binding and rearranging. *Trends Biochem. Sci. 36*, 19–29.

(3) Putnam, A. A., and Jankowsky, E. (2013) DEAD-box helicases as integrators of RNA, nucleotide and protein binding. *Biochim. Biophys. Acta 1829*, 884–893.

(4) Shibuya, T., Tange, T. O., Sonenberg, N., and Moore, M. J. (2004) eIF4AIII binds spliced mRNA in the exon junction complex and is essential for nonsense-mediated decay. *Nat. Struct. Mol. Biol. 11*, 346–351.

(5) Ballut, L., et al. (2005) The exon junction core complex is locked onto RNA by inhibition of eIF4AIII ATPase activity. *Nat. Struct. Mol. Biol. 12*, 861–869.

(6) Rozovsky, N., Butterworth, A. C., and Moore, M. J. (2008) Interactions between eIF4AI and its accessory factors eIF4B and eIF4H. *RNA 14*, 2136–2148.

(7) Nashchekin, D., Zhao, J., Visa, N., and Daneholt, B. (2006) A novel Ded1-like RNA helicase interacts with the Y-box protein ctYB-1 in nuclear mRNP particles and in polysomes. *J. Biol. Chem. 281*, 14263–14272.

(8) Tarn, W. Y., and Chang, T. H. (2009) The current understanding of Ded1p/DDX3 homologs from yeast to human. *RNA Biol. 6*, 17–20.

(9) Le Hir, H., and Andersen, G. R. (2008) Structural insights into the exon junction complex. *Curr. Opin. Struct. Biol. 18*, 112–119.

(10) Nielsen, K. H., et al. (2008) Mechanism of ATP turnover inhibtion in the EJC. *RNA 15*, 67–75.

(11) Andersen, C. B., et al. (2006) Structure of the exon junction core complex with a trapped DEAD-box ATPase bound to RNA. *Science 313*, 1968–1972.

(12) Bono, F., Ebert, J., Lorentzen, E., and Conti, E. (2006) The crystal structure of the exon junction complex reveals how it maintains a stable grip on mRNA. *Cell 126*, 713–725.

(13) Cao, W., et al. (2011) Mechanism of Mss116 ATPase reveals functional diversity of DEAD-Box proteins. *J. Mol. Biol. 409*, 399–414.

(14) Henn, A., Bradley, M. J., and De La Cruz, E. M. (2012) ATP utilization and RNA conformational rearrangement by DEAD-box proteins. *Annu. Rev. Biophys. 41*, 247–267.

(15) Yang, Q., and Jankowsky, E. (2005) ATP- and ADP-dependent modulation of RNA unwinding and strand annealing activities by the DEAD-box protein DED1. *Biochemistry 44*, 13591–13601.

(16) Halls, C., et al. (2007) Involvement of DEAD-box Proteins in Group I and Group II Intron Splicing. Biochemical Characterization of Mss116p, ATP Hydrolysis-dependent and -independent Mechanisms, and General RNA Chaperone Activity. *J. Mol. Biol. 365*, 835–855.

(17) Jankowsky, E., Gross, C. H., Shuman, S., and Pyle, A. M. (2000) The DExH protein NPH-II is a processive and directional motor for unwinding RNA. *Nature 403*, 447–451.

(18) Ha, T. (2001) Single-molecule fluorescence resonance energy transfer. *Methods 25*, 78–86.

(19) Liu, F., Putnam, A., and Jankowsky, E. (2008) ATP hydrolysis is required for DEAD-box protein recycling but not for duplex unwinding. *Proc. Natl. Acad. Sci. U. S. A. 105*, 20209–20214.

(20) Zhuang, X., et al. (2000) A single-molecule study of RNA catalysis and folding. *Science 288*, 2048–2051.

(21) Rasnik, I., McKinney, S. A., and Ha, T. (2005) Surfaces and orientations: much to FRET about? *Acc. Chem. Res. 38*, 542–548.

(22) Yang, Q., Fairman, M. E., and Jankowsky, E. (2007) DEAD-box-protein-assisted RNA structure conversion towards and against thermodynamic equilibrium values. *J. Mol. Biol. 368*, 1087–1100.

(23) Iost, I., Dreyfus, M., and Linder, P. (1999) Ded1p, a DEAD-box protein required for translation initiation in Saccharomyces cerevisiae, is an RNA helicase. *J. Biol. Chem. 274*, 17677–17683.

(24) Hilliker, A., Gao, Z., Jankowsky, E., and Parker, R. (2011) The DEAD-box protein Ded1 modulates translation by the formation and resolution of an eIF4F-mRNA complex. *Mol. Cell 43*, 962–972.

(25) Bowers, H. A., et al. (2006) Discriminatory RNP remodeling by the DEAD-box protein DED1. *RNA 12*, 903–912.

(26) Fairman, M., et al. (2004) Protein displacement by DExH/D RNA helicases without duplex unwinding. *Science 304*, 730–734.

(27) Gu, M., and Rice, C. M. (2010) Three conformational snapshots of the hepatitis C virus NS3 helicase reveal a ratchet translocation mechanism. *Proc. Natl. Acad. Sci. U.S.A. 107*, 521–528.

(28) Del Campo, M., and Lambowitz, A. M. (2009) Structure of the Yeast DEAD box protein Mss116p reveals two wedges that crimp RNA. *Mol. Cell 35*, 598–609.

(29) Montpetit, B., et al. (2011) A conserved mechanism of DEAD-box ATPase activation by nucleoporins and InsP6 in mRNA export. *Nature 472*, 238–242.

(30) Aregger, R., and Klostermeier, D. (2009) The DEAD box helicase YxiN maintains a closed conformation during ATP hydrolysis. *Biochemistry 48*, 10679–10681.

(31) Singleton, M. R., Dillingham, M. S., and Wigley, D. B. (2007) Structure and mechanism of helicases and nucleic acid translocases. *Annu. Rev. Biochem. 76*, 23–50.

(32) Putnam, A. A., and Jankowsky, E. (2013) AMP Sensing by DEAD-Box RNA Helicases. *J. Mol. Biol. 425*, 3839–3845.

(33) Theissen, B., Karow, A. R., Koehler, J., Gubaev, A., and Klostermeier, D. (2008) Cooperative binding of ATP and RNA induces a closed conformation in a DEAD-box RNA helicase. *Proc. Natl. Acad. Sci. U. S. A. 105*, 548–553.

(34) Yang, Q., Del Campo, M., Lambowitz, A. M., and Jankowsky, E. (2007) DEAD-box proteins unwind duplexes by local strand separation. *Mol. Cell 28*, 253–263.

(35) Henn, A., Cao, W., Hackney, D. D., and De La Cruz, E. M. (2008) The ATPase cycle mechanism of the DEAD-box rRNA helicase, DbpA. *J. Mol. Biol. 377*, 193–205.

(36) Henn, A., et al. (2010) Pathway of ATP utilization and duplex rRNA unwinding by the DEAD-box helicase, DbpA. *Proc. Natl. Acad. Sci. U.S.A. 107*, 4046–4050.

(37) Chen, Y., et al. (2008) The DEAD-box Protein CYT-19 Uses a Single ATP to Completely Separate a Short RNA Duplex. *Proc. Natl. Acad. Sci. U. S. A. 105*, 20203–20208.

(38) Shibuya, H., Kondo, K., Kimura, N., and Maruta, S. (2002) Formation and characterization of kinesin.ADP.fluorometal complexes. *J. Biochem. 132*, 573–579.

(39) Maruta, S., Henry, G. D., Sykes, B. D., and Ikebe, M. (1993) Formation of the stable myosin-ADP-aluminum fluoride and myosin-ADP-beryllium fluoride complexes and their analysis using $^{19}F$ NMR. *J. Biol. Chem. 268*, 7093−7100.
(40) Levin, M. K., Gurjar, M. M., and Patel, S. S. (2003) ATP binding modulates the nucleic acid affinity of hepatitis C virus helicase. *J. Biol. Chem. 278*, 23311−23316.
(41) Lee, J. Y., and Yang, W. (2006) UvrD helicase unwinds DNA one base pair at a time by a two-part power stroke. *Cell 127*, 1349−1360.
(42) Huang, H. R., et al. (2005) The splicing of yeast mitochondrial group I and group II introns requires a DEAD-box protein with RNA chaperone function. *Proc. Natl. Acad. Sci. U. S. A. 102*, 163−168.
(43) Rougemaille, M., et al. (2007) Dissecting mechanisms of nuclear mRNA surveillance in THO/sub2 complex mutants. *EMBO J. 26*, 2317−2326.
(44) Zhang, M., and Green, M. R. (2001) Identification and characterization of yUAP/Sub2p, a yeast homolog of the essential human pre-mRNA splicing factor hUAP56. *Genes Dev. 15*, 30−35.
(45) Saguez, C., et al. (2013) Mutational analysis of the yeast RNA helicase Sub2p reveals conserved domains required for growth, mRNA export, and genomic stability. *RNA 19*, 1363−1371.
(46) Zhao, R., Shen, J., Green, M. R., MacMorris, M., and Blumenthal, T. (2004) Crystal structure of UAP56, a DExD/H-box protein involved in pre-mRNA splicing and mRNA export. *Structure 12*, 1373−1381.
(47) Shi, H., Cordin, O., Minder, C. M., Linder, P., and Xu, R. M. (2004) Crystal structure of the human ATP-dependent splicing and export factor UAP56. *Proc. Natl. Acad. Sci. U. S. A. 101*, 17628−17633.
(48) Wong, I., and Lohman, T. M. (1997) A two-site mechanism for ATP hydrolysis by the asymmetric Rep dimer P2S as revealed by site-specific inhibition with ADP-AlF4. *Biochemistry 36*, 3115−3125.
(49) Fairman-Williams, M. E., and Jankowsky, E. (2012) Unwinding initiation by the viral RNA helicase NPH-II. *J. Mol. Biol. 415*, 819−832.
(50) Ali, J. A., and Lohman, T. M. (1997) Kinetic measurement of the step size of DNA unwinding by *Escherichia coli* UvrD helicase. *Science 275*, 377−380.
(51) Palmgren, M. G., and Nissen, P. (2011) P-type ATPases. *Annu. Rev. Biophys. 40*, 243−266.
(52) English, B. P., et al. (2006) Ever-fluctuating single enzyme molecules: Michaelis-Menten equation revisited. *Nat. Chem. Biol. 2*, 87−94.
(53) Fairman-Williams, M. E., Guenther, U. P., and Jankowsky, E. (2010) SF1 and SF2 helicases: family matters. *Curr. Opin. Struct. Biol. 20*, 313−324.